Available online at www.sciencedirect.com
ScienceDirect
Ceramics International 34 (2008) 849–852
CERAMICS INTERNATIONAL
www.elsevier.com/locate/ceramint

Fabrication and thermoelectric properties of heavily rare-earth metal-doped $SrO(SrTiO_3)_n$ ($n = 1, 2$) ceramics

Yi Feng Wang [a], Kyu Hyoung Lee [b], Hiromichi Ohta [a,b], Kunihito Koumoto [a,b,*]

[a] *Nagoya University, Graduate School of Engineering, Furo-cho, Chikusa, Nagoya 464-8603, Japan*
[b] *CREST, Japan Science and Technology Agency, 4-1-8 Honcho, Kawaguchi 332-0012, Japan*

Available online 29 September 2007

Abstract

To clarify the effect of substitutional electron doping on the thermoelectric figure of merit ($ZT = S^2\sigma T\kappa^{-1}$) of Ruddlesden–Popper phase $SrO(SrTiO_3)_n$ (or $Sr_{n+1}Ti_nO_{3n+1}$), measurements were conducted for several thermoelectric parameters, e.g. electrical conductivity (σ), Seebeck coefficient (S) and thermal conductivity (κ), of $(Sr_{1-x}RE_x)_{n+1}Ti_nO_{3n+1}$ ($n = 1$ or 2, RE (rare earth): La or Nd, $x = 0.05$ and 0.1) dense ceramics prepared by a conventional solid-state reaction and hot-pressing technique. Crystal structures of the resultant ceramics were represented as $(Sr_{1-x}RE_x)_{n+1}$ Ti_nO_{3n+1} evaluated by powder X-ray diffraction followed by the Rietveld analysis. All the ceramics exhibited electrical conductivity and the σ values simply depended on the dopant concentration, indicating that both La^{3+} and Nd^{3+} ions act as electron donors. The $|S|$ values increased with temperature due to decrease in the chemical potential. Significant reduction of the κ values was observed as compared to cubic-perovskite $SrTiO_3$. The ZT value increased with temperature and reached 0.15 at 1000 K for $(Sr_{0.95}La_{0.05})_3Ti_2O_7$.

Keywords: D. Perovskite; D. Transitional metal oxides; X-ray diffraction; Thermoelectric properties

1. Introduction

Thermoelectric (TE) materials can directly convert temperature difference between both ends of a solid into electric power due to the Seebeck effect [1]. Although several TE materials containing heavy metals such as Bi, Sb, Pb and Te have been developed so far [2–7], these materials are mostly toxic and unstable at high temperatures (~1000 K). Therefore, metal oxides which exhibit good TE performance, are strongly demanded because metal oxides are environmental friendly and basically stable at high temperatures. Recently, the authors found that heavily electron-doped $SrTiO_3$ exhibits a rather large TE figure of merit ($ZT = S^2\sigma T\kappa^{-1}$, S: Seebeck coefficient, σ: electrical conductivity, T: absolute temperature, and κ: thermal conductivity) of 0.37 at 1000 K [8,9], which is the largest among n-type metal oxide reported to date [10–13]. However, the performance is still low as compared to that of the state-of-the-art TE materials such as Bi_2Te_3 due to the fact that the κ value of $SrTiO_3$ (12 Wm^{-1} K^{-1} at 300 K [9]) is approximately one order of magnitude larger than that of Bi_2Te_3.

In order to efficiently reduce the κ value of $SrTiO_3$, focus is given on its layered perovskite-type $SrO(SrTiO_3)_n$ or $Sr_{n+1}Ti_nO_{3n+1}$ (n = integer) termed as Ruddlesden–Popper (RP) phases [14,15], which have a layered structure composed of alternate stacks of rock salt SrO layer and perovskite $(SrTiO_3)_n$ block layer along the c-axis. This is a candidate TE material because heavily electron-doped $SrO(SrTiO_3)_n$ can exhibit rather lower κ values because phonon scattering occurs efficiently at the interface between SrO layer and $(SrTiO_3)_n$ block layer, while it exhibits similar electron transport properties. Very recently, the authors reported that $SrO(SrTi_{1-x}Nb_xO_3)_n$ exhibits lower κ values as compared to $SrTiO_3$ [16]. In this study, $(Sr_{1-x}RE_x)_{n+1}Ti_nO_{3n+1}$ ($n = 1$ or 2, RE (rare earth): La or Nd, $x = 0.05$ and 0.1) dense ceramics were fabricated to compare TE properties with Nb-doped $SrTiO_3$ and $SrO(SrTi_{1-x}Nb_xO_3)_n$.

2. Fabrication of $Sr_{n+1}Ti_nO_{3n+1}$ ($n = 1, 2$) ceramics

$(Sr_{1-x}RE_x)_{n+1}Ti_nO_{3n+1}$ ($n = 1$ or 2, RE: La or Nd, $x = 0.05$ and 0.1) powders were prepared by conventional solid-state

* Corresponding author at: Graduate School of Engineering, Nagoya University, Nagoya 464-8603, Japan. Tel.: +81 52 789 3327; fax: +81 52 789 3201.
E-mail address: Koumoto@apchem.nagoya-u.ac.jp (K. Koumoto).

0272-8842/$34.00
doi:10.1016/j.ceramint.2007.09.034

Table 1
Distance of the Ti–O(1–3) and Ti–Ti, and the angle of the O(1)–Ti–O(1) bond of $(Sr_{1-x}RE_x)_{n+1}Ti_nO_{3n+1}$ ($n = 1$ or 2, *RE*: La or Nd, $x = 0.05$ and 0.1)

n	Dopant (at.%)		Bond length or atom distance (Å)				Bond angle (°)
			Ti–O(1)	Ti–O(2)	Ti–O(3)	Ti–Ti[1 1 0]	O(1)–Ti–O(1)
1	5	La	1.9444	1.9989	–	5.4997	180
		Nd	1.9440	1.9788	–	5.4985	180
2	5	La	1.9512	1.9028	2.0064	5.5184	178.57
		Nd	1.9502	1.8213	2.0138	5.5133	176.42
	10	La	1.9524	1.9262	2.0161	5.5210	177.62
		Nd	1.9480	1.7973	1.9955	5.5092	178.33

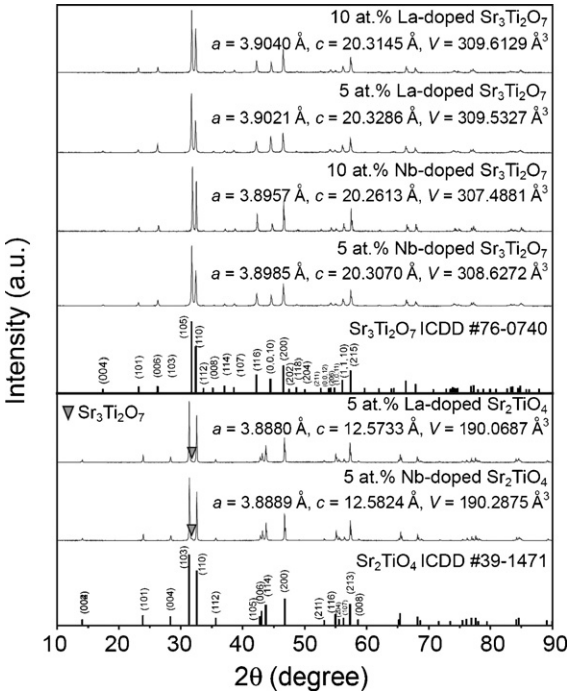

Fig. 1. Powder X-ray diffraction patterns for $(Sr_{1-x}RE_x)_{n+1}Ti_nO_{3n+1}$ ($n = 1$ or 2, *RE*: La or Nd, $x = 0.05$ and 0.1). Lattice parameters and volumes evaluated by least square method are also shown.

Table 2
Crystallographic data for $(Sr_{1-x}RE_x)_2TiO_4$ ($n = 1$) (*RE*: La or Nd, $x = 0$ and 0.05) (SG *I*4/*mmm*; no. 139)

Atom	Position	*x*	*y*	*z*	Dopant
Sr	4*e*	0	0	0.3541(1)	
				0.3545(2)	(La)
				0.3546(6)	(Nd)
Ti	2*a*	0	0	0	
O(1)	4*c*	0	0.5	0	
O(2)	4*e*	0	0	0.1568(9)	
				0.1588(6)	(La)
				0.1573(8)	(Nd)

R_{wp} (%)	R_p (%)	*S*	
13.14	8.98	2.2164	(La)
12.28	8.81	1.3663	(Nd)
11.63	8.92	1.8744	

reaction of the stoichiometric mixture of $SrCO_3$, TiO_2 (rutile), La_2O_3 and Nd_2O_3 powders. Starting powders were mixed for 1 h in a planetary ball mill and calcined for 12 h at 1200 °C in air. The powder was heated at 1400–1425 °C for 1 h in a carbon crucible under an Ar atmosphere, in order to form the RP phases and generate the electron carriers through the reduction of Ti^{4+} to Ti^{3+} by doping of RE^{3+}. After further ball milling, highly dense polycrystalline ceramic samples were fabricated by conventional hot pressing (36 MPa and 1400–1425 °C for 1 h in an Ar flow).

Table 3
Crystallographic data for $(Sr_{1-x}RE_x)_3Ti_2O_7$ ($n = 2$) (*RE* = La or Nd, $x = 0$–0.1) (SG *I*4/*mmm*; no. 139)

Atom	Position	*x*	*y*	*z*	Dopant
Sr(1)	4*e*	0.5	0.5	0	
Sr(2)	2*b*	0.5	0.5	0.1854(4)	Undoped
				0.1853	a
				0.1848(6)	b
				0.1859	c
				0.1850	d
Ti	4*e*	0	0	0.0985(5)	Undoped
				0.0987	a
				0.0992(4)	b
				0.0991(7)	c
				0.0984(9)	d
O(1)	8*g*	0.5	0	0.0961(6)	Undoped
				0.0975	a
				0.0972	b
				0.0961(8)	c
				0.0970(6)	d
O(2)	4*e*	0	0	0.1908(5)	Undoped
				0.1923	a
				0.1940(6)	b
				0.1888(6)	c
				0.1872	d
O(3)	2*a*	0	0.5	0	

R_{wp} (%)	R_p (%)	*S*	
11.63	8.92	1.8744	
14.05	170.92	1.79	[a] $(Sr_{0.95}La_{0.05})_3Ti_2O_7$
13.35	10.72	1.75	[b] $(Sr_{0.9}La_{0.1})_3Ti_2O_7$
11.63	8.92	1.8744	[c] $(Sr_{0.95}Nd_{0.05})_3Ti2O_7$
15.69	11.69	1.3304	[d] $(Sr_{0.9}Nd_{0.1})_3Ti_2O_7$

3. Results and discussion

3.1. Crystallographic characterization

Powder X-ray diffraction (XRD) patterns of the resultant ceramics (Fig. 1) revealed that the resultant $n = 2$ $(Sr_{1-x}RE_x)_3Ti_2O_7$ ceramics were single phase and the $n = 1$ $(Sr_{1-x}RE_x)_2TiO_4$ samples were mixed with a secondary phase of $(Sr_{1-x}RE_x)_3Ti_2O_7$, suggesting the high stability of $n = 2$ RP phase, $Sr_3Ti_2O_7$ among the RP phases. Rietveld refinement was also conducted based on the space group *I*4/*mmm* (no. 139) by using the RIETAN 2000 program [17] for further analysis of the crystal structure. The reliability factor R_{wp} was ~10% in all compounds, and the obtained crystallographic data are given in Fig. 1 and Tables 1–3; details of the structural features of $Sr_{n+1}Ti_nO_{3n+1}$ ($n = 1, 2$) are described in a previous report [16]. It should be noted that the resultant ceramics were fully dense (95–98% of theoretical density) to measure the TE properties, and almost no pores can be observed in SEM images (Fig. 2), which were taken after chemical etching in a diluted HF solution for 1 min.

3.2. Thermoelectric properties

Measurements of S and σ values for the $(Sr_{1-x}RE_x)_{n+1}Ti_nO_{3n+1}$ ceramic samples were performed simultaneously by a conventional steady-state method and a d.c. four probe method, respectively, in Ar atmosphere in the temperature range from 300 to 1000 K. The κ values of the dense $(Sr_{1-x}RE_x)_{n+1}Ti_nO_{3n+1}$ ceramics were calculated as $\kappa = a\ \rho\ C_p$ using the values of thermal diffusivity (a) and heat capacity (C_p), which were separately measured by the laser-flash method under vacuum and differential scanning calorimetry (DSC) in air, respectively.

All the $(Sr_{1-x}RE_x)_{n+1}Ti_nO_{3n+1}$ ceramics exhibited electrical conductivity and the σ values simply depended on the dopant concentration, indicating that both La^{3+} and Nd^{3+} ion fully act as an electron donor (Fig. 3a). Since all the ceramic samples were degenerate semiconductor, the σ values decrease with temperature because a reduction of electron mobility occurs due to phonon scattering [9]. On the other hand, below 700 K, the temperature dependence of σ is not linear, implying that the grain boundary scattering is still dominant in this temperature range due to the presence of grain boundaries as shown in Fig. 2. All samples have negative S, indicating that the samples

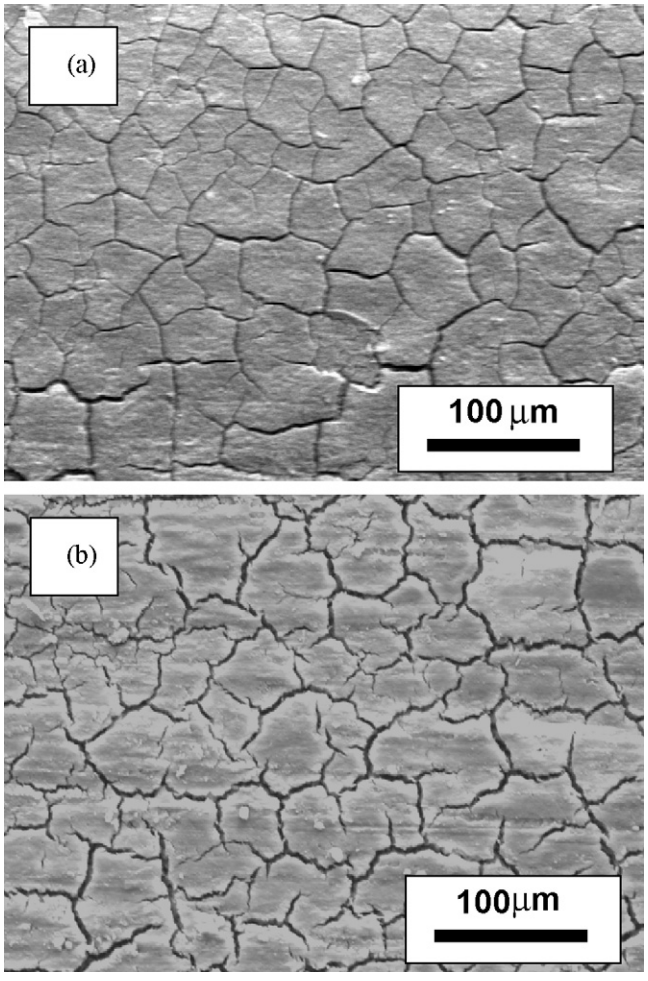

Fig. 2. SEM micrographs of hot-pressed (a) $(Sr_{0.95}La_{0.05})_3Ti_2O_7$ and (b) $(Sr_{0.95}Nd_{0.05})_3Ti_2O_7$, polished and chemically etched with a diluted HF solution.

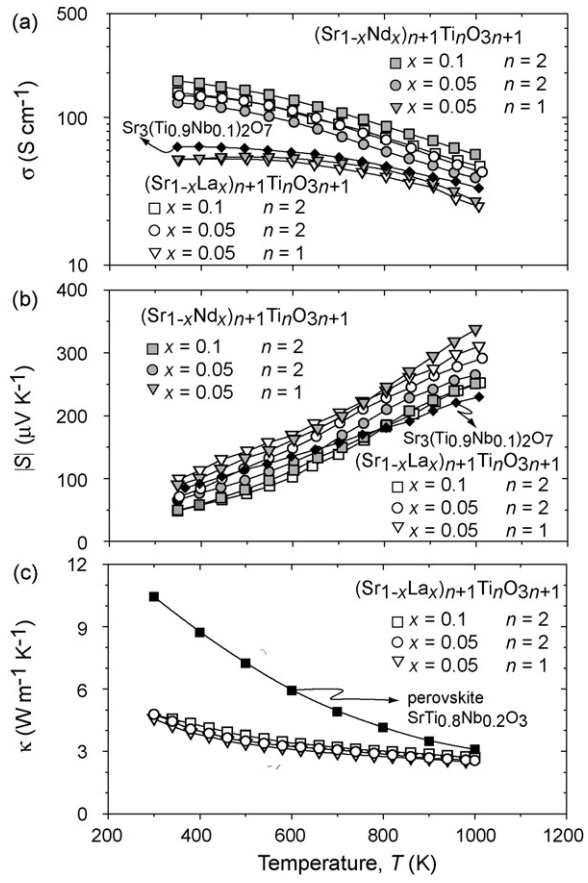

Fig. 3. Temperature dependence of (a) electrical conductivities (σ), (b) Seebeck coefficients (S), and (c) thermal conductivities (κ) of $(Sr_{1-x}RE_x)_{n+1}Ti_nO_{3n+1}$ ($n = 1$ or 2, *RE*: La or Nd, $x = 0.05$ and 0.1). Data for 10 at.% Nb-doped $Sr_3Ti_2O_7$ ($n = 2$) polycrystalline samples shown in (a) and (b) are taken from Ref. [16] (filled diamonds) and κ values for 20 at.% Nb-doped $SrTiO_3$ ($n = \infty$) polycrystalline samples shown in (c) are taken from Ref. [9] (filled squares).

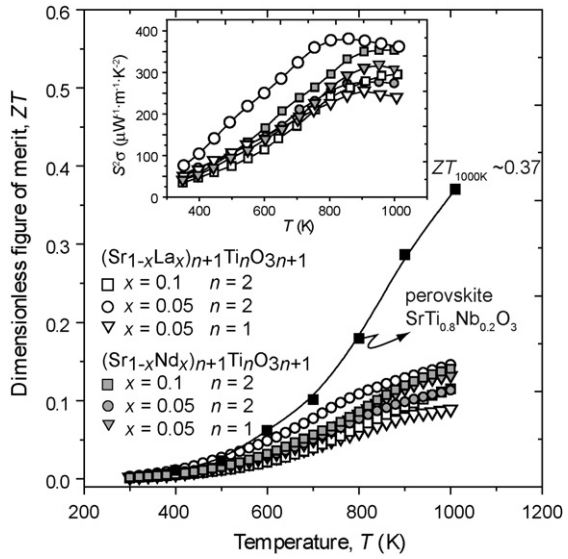

Fig. 4. Temperature dependence of ZT values and the power factors (inset) for $(Sr_{1-x}RE_x)_{n+1}Ti_nO_{3n+1}$ ($n = 1$ or 2, RE: La or Nd, $x = 0.05$ and 0.1). Data for 20 at.% Nb-doped $SrTiO_3$ ($n = \infty$) polycrystalline samples are taken from Ref. [9] (filled diamonds).

are n-type degenerate semiconductors, and the $|S|$ values of all samples increased with temperature due to decrease of the chemical potential (Fig. 3b). Significant reduction of the κ values was observed as compared to cubic perovskite $SrTiO_3$ (Fig. 3c). The total thermal conductivity (κ_{tot}) is represented as the sum of electronic (κ_{ele}) and lattice contributions (κ_{lat}). In the present case, κ_{ele} increases with increasing RE content owing to the increase in carrier concentration, however, the κ_{ele} values estimated by use of the Wiedemann–Franz law are very small ($\kappa_{ele} \sim 0.3\ W\ m^{-1}\ K^{-1}$) as compared to κ_{tot}, which indicates that the phonon contribution is predominant. Thus, the reduction in thermal conductivity is considered to be due to the phonon scattering at $SrO/(SrTiO_3)_n$ interfaces of the inherent superlattice structure.

From σ, S and κ values, the power factor ($S^2\sigma$) and the dimensionless figure of merit, ZT ($S^2\sigma T\kappa^{-1}$) of the $(Sr_{1-x}RE_x)_{n+1}Ti_nO_{3n+1}$ ceramics were calculated (Fig. 4). The maximum power factor value is $378.1\ \mu W^{-1}\ m^{-1}\ K^{-2}$ for $(Sr_{0.95}La_{0.05})_3Ti_2O_7$ (inset of Fig. 4) which is ~30% of that of perovskite-type Nb-doped $SrTiO_3$, and the ZT values increase with temperature in all compositions and reaches ~0.15 at 1000 K, which is similar to that of $SrO(SrTi_{1-x}Nb_xO_3)_n$ [16]. From these results, it is concluded that the doping effect of La^{3+} and Nd^{3+} is basically similar to that of Nb^{5+} on TE properties of $SrO(SrTiO_3)_n$ ($n = 1, 2$). Although significant reduction of κ values was achieved in $SrO(SrTiO_3)_n$ ($n = 1, 2$), the ZT value is lower than that of $SrTi_{0.8}Nb_{0.2}O_3$ ($ZT_{1000\ K} = 0.37$) [8,9].

4. Summary

Several thermoelectric parameters such as electrical conductivity (σ), Seebeck coefficient (S) and thermal conductivity (κ) were measured for $(Sr_{1-x}RE_x)_{n+1}Ti_nO_{3n+1}$ ($n = 1$ or 2, RE: La or Nd, $x = 0.05$ and 0.1) dense ceramics, which were prepared by a conventional solid-state reaction and hot-pressing technique to compare their thermoelectric properties with Nb-doped $SrTiO_3$ and $SrO(SrTi_{1-x}Nb_xO_3)_n$. The $(Sr_{1-x}RE_x)_{n+1}Ti_nO_{3n+1}$ ceramics exhibited similar thermoelectric properties to those of $SrO(SrTi_{1-x}Nb_xO_3)_n$, indicating that the dopant ions (La^{3+} and Nd^{3+}) act as a donor, while they do not significantly affect the density of states for the conduction band.

Acknowledgments

The authors sincerely thank Dr. Hideki Kita and Dr. Hideki Hyuga of the National Institute of Advanced Industrial Science and Technology (AIST), Japan for their technical assistance in hot pressing. The authors would also like to thank Dr. Kouta Iwasaki (Nagoya Univ.) for instructive discussion on the Rietveld refinement.

References

[1] C.B. Vining, Semiconductors are cool, Nature 413 (2001) 577–578.
[2] D.Y. Chung, T.P. Hogan, P. Brazis, M. Rocci-Lane, C. Kannewurf, M. Bastea, C. Uher, M.G. Kanatzidis, $CsBi_4Te_6$: a high-performance thermoelectric material for low-temperature applications, Science 287 (2000) 1024–1027.
[3] D.A. Wright, Thermoelectric properties of bismuth telluride and its alloys, Nature 181 (1958) 834.
[4] D.A. Polvani, J.F. Meng, N.V.C. Shekar, J. Sharp, J.V. Badding, Large improvement in thermoelectric properties in pressure-tuned p-type $Sb_{1.5}Bi_{0.5}Te_3$, Chem. Mater. 13 (2001) 2068–2071.
[5] W.M. Yim, A. Amith, Bi–Sb alloys for magneto-thermoelectric and thermomagnetic cooling, Solid State Electron. 15 (1972) 1141–1144.
[6] G.J. Snyder, J.R. Lim, C. Huang, J. Fleurial, Thermoelectric microdevice fabricated by a MEMS-like electrochemical process, Nat. Mater. 2 (2003) 528–531.
[7] X.H. Ji, X.B. Zhao, Y.H. Zhang, B.H. Lu, H.L. Ni, Synthesis and properties of rare earth containing Bi_2Te_3 based thermoelectric alloys, J. Alloys Compd. 387 (2005) 282–286.
[8] S. Ohta, T. Nomura, H. Otha, M. Hirano, H. Hosono, K. Koumoto, Large thermoelectric performance of heavily Nb-doped $SrTiO_3$ epitaxial film at high temperature, Appl. Phys. Lett. 87 (2005) 092108.
[9] S. Ohta, H. Ohta, K. Koumoto, Grain size dependence of thermoelectric performance of Nb-doped $SrTiO_3$ polycrystals, J. Ceram. Soc. Jpn. 114 (2006) 102–105.
[10] M. Yasukawa, N. Murayama, A promising oxide material for high-temperature thermoelectric energy conversion: $Ba_{1-x}Sr_xPbO_3$ solid solution system, Mater. Sci. Eng. B 54 (1998) 64–69.
[11] K. Park, K.Y. Ko, W.S. Seo, W.S. Cho, J.G. Kim, J.Y. Kim, High-temperature thermoelectric properties of polycrystalline $Zn_{1-x-y}Al_xTi_yO$ O ceramics, J. Eur. Ceram. Soc. 27 (2007) 813–817.
[12] D. Kurita, S. Ohta, K. Sugiura, H. Ohta, K. Koumoto, J. Appl. Phys. 100 (2006) 096105.
[13] K.F. Cai, E. Müller, C. Drašar, A. Mrotzek, Preparation and thermoelectric properties of Al-doped ZnO ceramics, Mater. Sci. Eng. B 104 (2003) 45–48.
[14] S.N. Ruddlesden, P. Popper, New compounds of the K_2NiF_4 type, Acta Crystallogr. 10 (1957) 538–539.
[15] S.N. Ruddlesden, P. Popper, The compound $Sr_3Ti_2O_7$ and its structure, Acta Crystallogr. 11 (1958) 54–55.
[16] K.H. Lee, S.W. Kim, H. Ohta, K. Koumoto, Ruddlesden–Popper phases as thermoelectric oxides: Nb-doped $SrO(SrTiO_3)_n$ ($n = 1, 2$), J. Appl. Phys. 100 (2006) 063717.
[17] F. Izumi, T. Ikeda, A Rietveld-analysis program RIETAN-98 and its applications to zeolites, Mater. Sci. Forum 321 (2000) 198–203.